European Journal of Cell Biology 98 (2019) 151045

Contents lists available at ScienceDirect

European Journal of Cell Biology

journal homepage: www.elsevier.com/locate/ejcb

Research paper

An improved cellular enucleation method with extracellular matrix and colchicine facilitates the study of nucleocytoplasmic interaction

Yu Chen[a], Li-qun Xu[a], Mei-Jia Lin[a], Wei Zhang[a], Zhong-jian Zhang[b,*], Wen-can Xu[c], Lv-jun Yang[d], Chi-ju Wei[a,*]

[a] Multidisciplinary Research Center, Shantou University, Shantou, Guangdong 515063, China
[b] Institute of Psychiatry and Neuroscience, Xinxiang Medical University, Xinxiang, Henan, 453000, China
[c] Department of Endocrinology, The First Affiliated Hospital of Shantou University Medical College, Shantou, Guangdong 515041, China
[d] Department of Burn and Plastic Surgery, The Second Affiliated Hospital of Shantou University Medical College, Shantou, Guangdong 515041, China

ARTICLE INFO

Keywords:
Enucleation
Cytoplast
ECM
Mitochondria
Paclitaxel
Apoptosis

ABSTRACT

Enucleated mammalian cells (cytoplasts) have been widely used for studying differential roles of the cytoplasm and nucleus in various cellular processes. Here, we reported an improved enucleation protocol, in which cells were seeded in extracellular matrix (ECM)-coated 24-wells and spun at 4600 g and 35 °C for 60 min in the presence of cytochalasin B and colchicine. When glass-bottom wells were used, cellular structures and organelles in cytoplasts could be examined directly by confocal microscopy. Nuclear envelope rupture did not occur probably due to mild centrifugation conditions used in this study. Addition of paclitaxel or doxorubicin completely blocked proliferation of residual nucleated cells; however, to our surprise, paclitaxel dramatically prolonged the survival of cytoplasts. Results from Annexin V and Propidium Iodide staining showed that cytoplasts died predominantly by apoptosis, which was partially inhibited by ECM and further by paclitaxel. Mitochondria were mostly rod-shaped and formed a connected network in paclitaxel-treated cytoplasts, indicating lack of fusion and fission dynamics. Moreover, paclitaxel increased mitochondrial membrane potential, suggesting that perturbation of mitochondria might be critical to the survival of cytoplasts. In conclusion, we had established an efficient and fast procedure for enucleation of adherent animal cells, which could facilitate the investigation of nucleocytoplasmic interaction.

1. Introduction

Cytoplasts are enucleated cells that are useful for studying differential contributions of the cytoplasm and nucleus in various cellular processes. A recent study demonstrated that the nucleus is dispensable for polarization and migration in one-dimension (1D) and two-dimensions (2D) environment; however, it is critical for 3D migration and proper mechanical responses (Graham et al., 2018). Infection studies in enucleated host cells have confirmed that the nucleus is not required for the life cycle of some viral and non-viral pathogens (Follett et al., 1974; de Souza Carvalho et al., 2011). A Cisplatin-induced apoptotic signaling pathway (Mandic et al., 2003) and a nongenomic mechanism underlying cystic change in the endoplasmic reticulum (ER) (Lee et al., 2013) have been identified in cytoplasts. Further, it has been demonstrated that cytoplasmic activities alone are responsible for regulating tubulin biosynthesis (Caron et al., 1985).

Enucleated egg has profound applications including being used for mitochondrial replacement therapy (MTR). Although still ethically debated, however, the technique gives women carrying mtDNA mutations an excellent chance of having a genetically related child without the rick of passing on mitochondrial diseases (Herbert and Turnbull, 2018). On the contrary, there is no therapy available to cure patients with mtDNA diseases, which often lead to severe disability and death. It has been reported that a functional *ND4* gene could be transferred into mitochondria in a mouse model of Leber hereditary optic neuropathy (LHON) (Yu et al., 2012). However, the efficacy of mitochondrial gene therapy is unclear. Recently, we have reported the generation of plasma membrane vesicles, which are miniature enucleated cells, with the potential of curing mitochondrial diseases (Lin et al., 2016; Xu et al., 2017).

Cellular enucleation by centrifugation in the presence of cytochalasin B is a well-established technique reported initially in the 70 s of last century (Prescott et al., 1972; Wigler and Weinstein, 1975). Basically, the centrifugation could be performed with cells either adhered to

* Corresponding authors.
E-mail addresses: 15lqxu@stu.edu.cn (Z.-j. Zhang), chijuwei@stu.edu.cn (C.-j. Wei).

https://doi.org/10.1016/j.ejcb.2019.151045
Received 14 April 2019; Received in revised form 18 June 2019; Accepted 23 July 2019

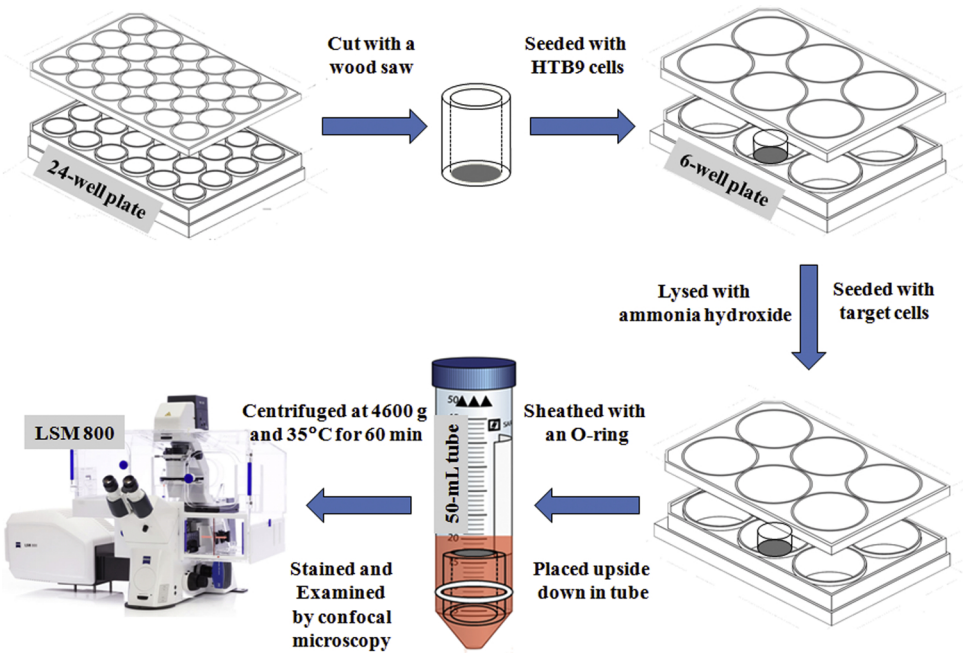

Fig. 1. Schematic of the cellular enucleation process. Step 1: Individual 24-well was cut out from the plate with a wood saw; Step 2: the 24-well was seeded with HTB9 cells and put into a 6-well plate and cultivated in an incubator; Step 3: ECM of HTB9 cells were prepared by ammonia lysis after 24–48 h cultivation. Cells to be enucleated were seeded; Step 4: After 24 h incubation, the 24-well was sheathed with a medical grade latex O-ring, and then put upside down into a 50-ml conical tube, which was pre-filled with 10 ml warm culture medium supplemented with cytochalasin B and/or colchicine, for enucleation by centrifugation at 6000 RPM (4600 *g*) and 35 °C for 60 min; Step 5: Enucleated cells were recovered in culture medium for more than 2 h, stained with dyes such as Calcein-AM and Hoechst, and then used for analysis by confocal microscopy.

a coverslip or suspended in a Ficoll/Percoll gradient. The first method is simple, but it is not easy to put or take the coverslip in and out of the centrifuge tube. Also, cells with poor adhesion capability are not enucleated efficiently. The latter method can generate larger quantity of cytoplasts, which however are not well separated from the karyoplasts and thus further purification is necessary.

Here, we reported an improved enucleation approach based on the classical coverslip method. Cells were seeded in a 24-well, which was pre-coated with extracellular matrix (ECM) from human bladder carcinoma HTB9 cells. The well was cut out and fitted into a 50-ml conical tube. A plastic O-ring was designed and used to position the 24-well in the conical tube. Cellular enucleation with high efficiency could be achieved at a relatively low centrifugal speed of 6000 RPM (about 4600 g) in the presence of cytochalasin B and colchicine. More importantly, cytoplasts generated in the presence of ECM had higher viabilities, which could facilitate the study of cytoplasm and nucleus interaction.

2. Materials and methods

2.1. Materials

Biochemical reagents, antibodies and plasmids were purchased from companies as indicated below: cytochalasin B, colchicine, paclitaxel and doxorubicin (Meilun, Dalian, China), TMRE (Solarbio, Beijing, China), Phalloidin-FITC (Yeasen, Shanghai, China), MitoTracker-Green, LysoTracker, Hoechst 33342, DCFH-DA and CM-DiI (Beyotime, Shanghai, China), Calcein-AM (Genesion, Guangzhou, China), DAPI (4′,6-diamidino-2-phenylindole, Dojindo, Japan), pLamin B-mCherry, pH2B-EGFP, pNLS-DsRed (Addgene, Cambridge, MA), Mouse monoclonal anti-α-tubulin (Sigma, St Louis, MO), Rabbit polyclonal anti-collagen I (Bioss, Beijing, China), Rabbit polyclonal anti-fibronectin (Proteintech, Wuhan, China), Alexa Fluor 555 Donkey anti Rabbit LgG (H + C) (Beyotime, Shanghai, China), Cy3 Sheep anti Mouse IgG (Sigma, St Louis, MO).

2.2. Preparation of ECM from HTB9 cells

Human bladder carcinoma HTB9 cells were propagated in Dulbecco's Modified Eagle Medium (DMEM, Life Technologies, Rockville, MD) supplemented with 10% fetal calf serum (HyCLONE, Logan, UT), 2 mM glutamine, 50 U/ml of penicillin G sodium and 50 mg/ml of streptomycin sulfate (Beyotime, Haimen, China). Cells were cultured in a humidified incubator at 37 °C supplied with 5% CO2. About 2×10^5/well of HTB9 cells were seeded in a 24-well (Corning), or a glass-bottom 24-well (NEST Biotechnology, Wuxi, China), and grew to 90% confluency after 48 h cultivation. ECM was then prepared by lysis with 20 mM ammonium hydroxide solution according to a reported protocol (Hellewell et al., 2017). Briefly, after removing culture medium and washing with PBS, 0.5 ml of ammonium solution was added into the 24-well. Incubate the well for 5 min with gentle agitation at every min. Wash the well with 1 ml of de-ionized H_2O twice followed by 1 ml of PBS. The well could be used immediately or stored in a refrigerator for up to 1 week.

2.3. ECM fluorescence staining

HTB9 cells and ECM were stained with anti-fibronectin and anti-collagen I antibodies. Cells were fixed with 4% paraformaldehyde for 10 min and permeabilized with 0.1% triton-X for 10 min at room temperature. Incubation of the primary antibodies was performed at room temperature for 2 h. Fluorescence conjugated secondary antibodies were added and incubated for 1 h. Wash with PBS three times after each step of incubation. Cell and ECM were examined under a confocal microscope (Zeiss LSM 800, Carl Zeiss, Germany).

2.4. ECM protein electrophoresis

ECM was harvested as described (Hellewell et al., 2017) and used for electrophoresis. Briefly, add 200 µl of pre-heat SDS-PAGE sample buffer containing 100 mM dithiothreitol (DTT) to a 10-cm dish. ECM was then collected with a cell scraper. ECM proteins were analyzed by SDS-PAGE using a 7% gradient polyacrylamide gel under reducing conditions. The gel was stained with Coomassie Blue.

2.5. ECM proteomic analysis

For proteomic analysis, ECM from multiple 10-cm dishes were collected with reused SDS-PAGE sample buffer to ensure the concentration was high enough for proteomic analysis. Harvested ECM was sent to

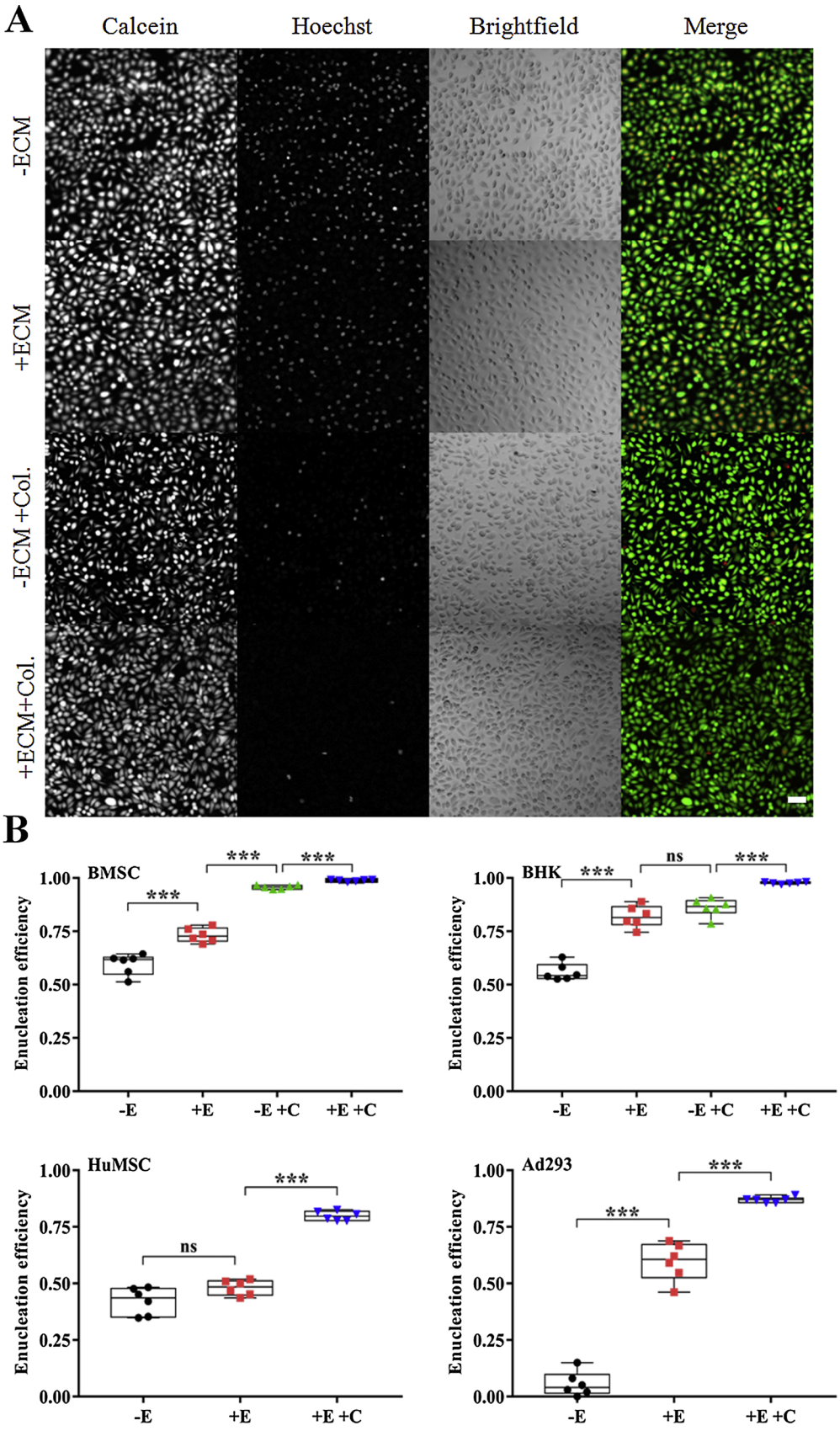

Fig. 2. Measurement of enucleation efficiency. (A) BMSCs were enucleated with or without ECM and supplementation of colchicine (Col.). Cells were stained with Calcein and Hoechst before being analyzed by confocal microscopy. Scale bar = 50 μm. (B) Boxplots of enucleation percentage for BMSCs (n = 6), BHKs (n = 6), HuMSCs (n = 6) and Ad293 cells (n = 6) after centrifugation with or without ECM and supplementation of colchicine. ECM: E; colchicine: C. ***, $P < 0.001$; **, $P < 0.01$; *, $P < 0.05$.

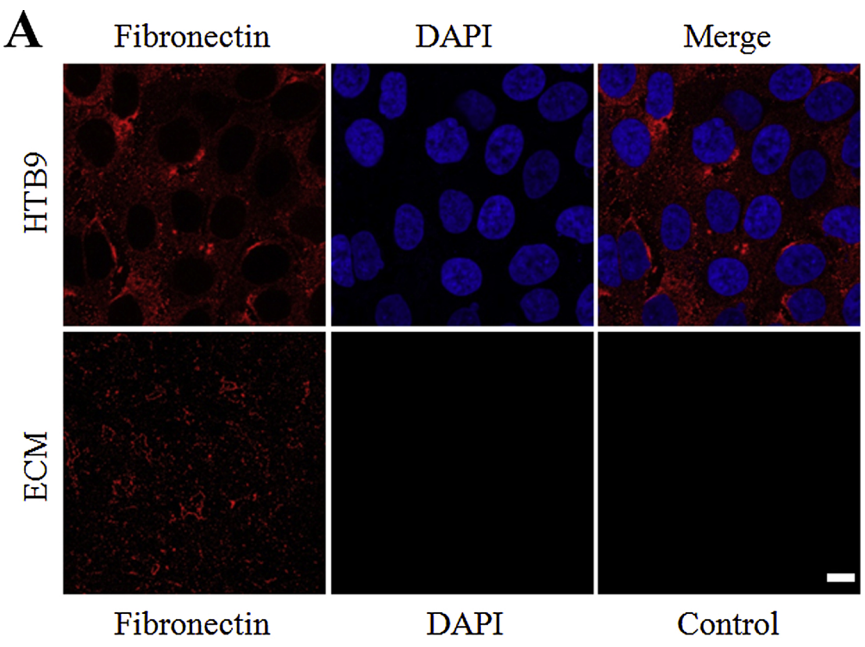

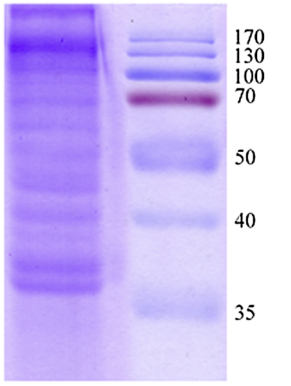

C

Protein identification	Unused ProtScore	No.Peptides/(Coverage)
Laminin subunit alpha-3	145.51	76 (22.65%)
Plectin	140.82	68 (19.06%)
Integrin beta-4	118.84	62(40.12%)
Laminin subunit beta-3	103.65	51(52.3%)
laminin subunit gamma-2	93.52	50 (47.86%)
Integrin alpha-6	91	49 (45.31%)
Annexin A2	88.38	49 (82.01%)
Transforming growth factor -beta-induced protein ig-h3	73.58	39 (62.08%)

Fig. 3. Analysis of protein components in ECM from HTB9 cells. (A) Detection of Fibronectin in HTB9 cells and ECM. HTB9 cells were cultivated in glass-bottom well from 48 h and lysed with ammonia solution to prepare ECM. Both HTB9 cells (top panel) and ECM (lower panel) were examined for the presence of fibronectin. After staining with DAPI, the samples were examined by confocal microscopy. Control: no primary antibody. Scale bar = 10 μm. (B) Electrophoresis and (C) Proteomics analysis of harvested ECM from HTB9 cells. Identity of cell-substrate interacting proteins within the top 15 Unused ProtScore are presented from one of two proteomics analysis using separate ECM preparations.

WuHan Genecreate Biological Engineering (China) and analyzed by liquid chromatography-tandem mass spectrometry (LC–MS/MS) using an AB SCIEX Triple TOF™ 5600 plus mass spectrometer after digestion with trypsin. The raw data were analyzed by comparison with known sequences using the ProteinPilot Software. A listing of the top 50 peptides was shown in Table S1 in Supplementary Materials.

2.6. Cell adhesion and proliferation analysis

BMSCs (Bone marrow mesenchymal stem cells, bought from Otwo Biotech, China), BHK (Baby hamster kidney)-21 cells, HuMSCs (human umbilical mesenchymal stem cells, provided by Dr. Yang of Shantou University Medical College) and Ad293 cells (derived from the standard Human Embryonic Kidney 293 cells) were seeded into ECM-coated and control 24-wells (2×10^5/well) and incubated at 37 °C for 30 min or 4 h. Individual 24-well was cut from the plate with a wood saw before cell seeding. The well was sheathed with a medical grade O-ring (inner diameter: 18 mm; outer diameter: 25 mm; thickness: 3 mm), which was purposely designed to position the 24-well evenly inside a 50-ml conical tube. The 24-well was placed upside down into the 50-ml tube, which was pre-filled with 10 ml of warm culture medium. Care was taken to prevent trapping of air bubbles inside the well. An Eppendorf centrifuge (5804R) with a fixed angle rotor (F-34-6-38) was pre-warmed to 35 °C by centrifugation. Cells were spun at 1000 rpm (130 g) and 35 °C for 5 min. After centrifugation, cells were stained with Hoechst (10 μg/ml) and Calcein-AM (2 μM) at 37 °C for 10 min. After washing with warm PBS twice, cells were examined under a confocal microscope (Zeiss LSM800) using a 10X objective. Image was analyzed with Image-Pro Plus 6.0. Cell number and area were calculated. For cell proliferation, cells (5×10^4/well) were seeded in 96-wells, which had been pre-coated with or without ECM. After incubation for 24 or 48 h, cell proliferation was measured by using the CCK8 kit according to the instruction.

2.7. Cellular enucleation

About 5×10^5/well of cells were seeded in an ECM coated 24-well and put into a 6-well plate. After 24–48 h cultivation, cells reached about 90% confluency. The well was sheathed with an O-ring, and then fitted into a 50-ml conical tube, which contained 10 ml warm culture medium supplemented with cytochalasin B (10 μg/ml) and/or colchicine (5 μg/ml). The 24-well was placed upside-down, and spun in a warm Eppendorf centrifuge at 6000 rpm (4600 *g*) and 35 °C for 60 min. The medium was replaced with fresh culture medium and the cells were recovered in the incubator for at least 2 h before being used for analysis.

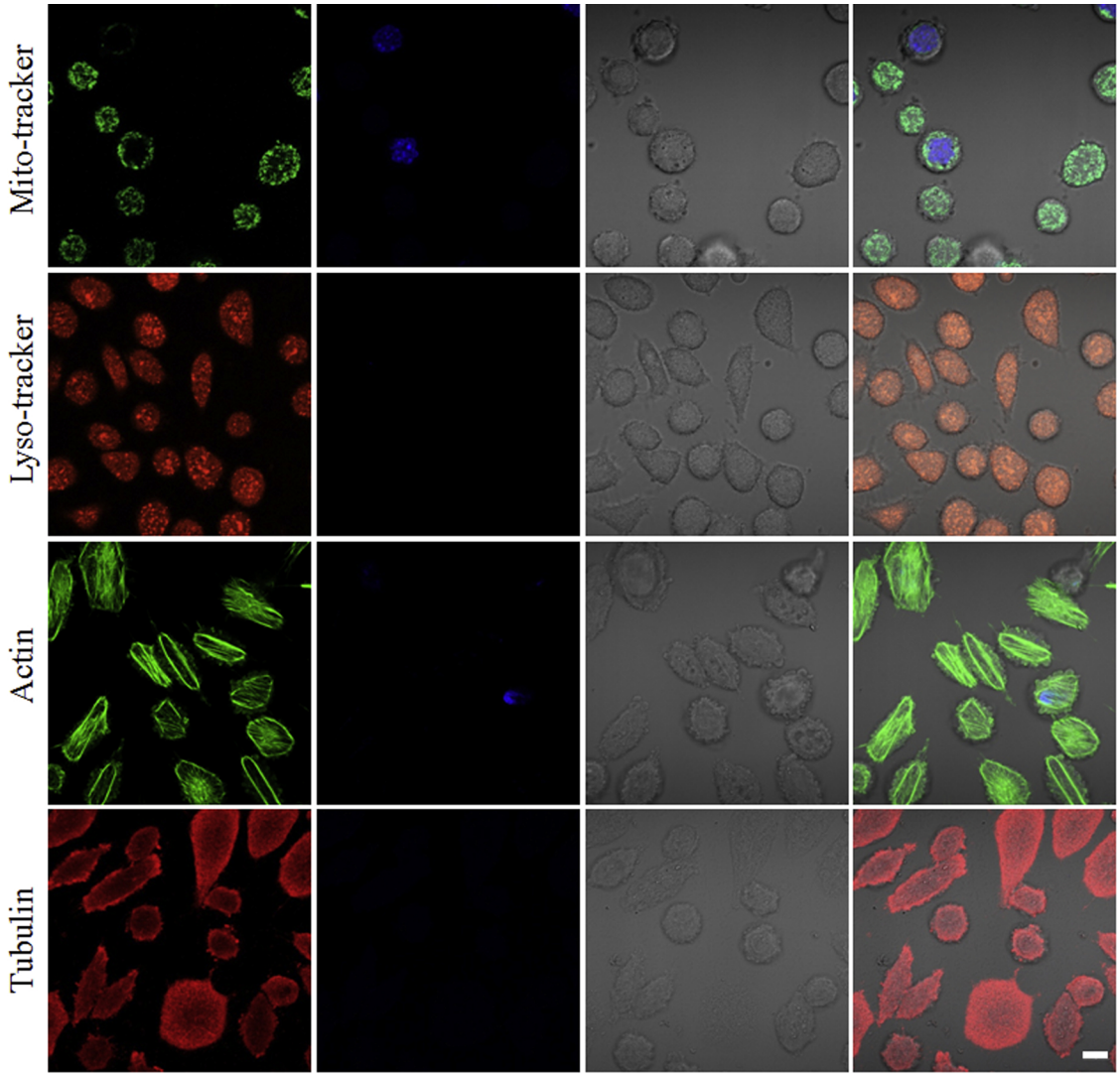

Fig. 4. Cellular enucleation in glass-bottom wells. BMSCs were seeded in an ECM-coated glass-bottom 24-well. After centrifugation at 7000 RPM (6300 *g*), cells were incubated with Mito-Tracker Green, or Lyso-Tracker Red to reveal mitochondria and lysosomes respectively by confocal microscopy. Alternatively, cells were fixed and incubated with Phalloidin-FITC or Anti-tubulin to detect microfilament and microtubule respectively. Scale bar = 10 μm.

2.8. Measurement of cytoplast viability

After enucleation as described above, cells were recovered in an incubator. At 2, 12, 24 and 36 h, the medium was removed and washed with warm PBS twice. Cells were stained with Calcein-AM (2 μM) for 10 min, washed with PBS and then stained with Hoechst (10 μg/ml) for 10 min. After washing, cells were examined under a confocal microscope using a 10X objective. Image was analyzed with Image-Pro Plus 6.0. Cells with or without a nucleus were counted.

2.9. Mitochondria and cytoskeleton staining

For fluorescence dye staining, cells with or without a nucleus were stained with Mito-Tracker Green (200 nM), TMRE (100 nM), or Lyso-Tracker Red (150 nM) at 37 °C for 30 min. After washing with warm PBS twice, cells were examined under a confocal microscope and analyzed with Image-Pro Plus 6.0.

For detection of actin filaments and microtubules, cells were fixed with 4% paraformaldehyde at room temperature for 10 min, and permeabilized with 01% triton-X for 10 min. After washing with PBS, cells were stained with Phalloidin-FITC or Mouse monoclonal anti-α-tubulin antibody for 2 h. For detection of microtubule, cells were further stained with Cy3 Sheep anti Mouse IgG for 1 h. After washing with PBS, cells were examined by confocal microscopy.

2.10. Measurement of ROS

Cytoplasts from BMSCs were harvested in PBS and loaded with DCFH-DA (10 μM) by static incubation for 20 min. Cytoplasts were washed three times with PBS, and then incubated with or without paclitaxel (25 μM) or doxorubicin (10 μM) for 30 min. Cytoplasts were immediately seeded into a 35-mm glass bottom dish (Corning, USA). and examined by confocal microscopy. Relative fluorescence intensity was calculated using the ZEN software.

2.11. Measurement of apoptosis

Cytoplasts from BMSCs in glass-bottom wells were cultivated with or without paclitaxel (25 μM) or doxorubicin (10 μM) for 36 h. Cytoplasts were stained with Annexin V-FITC (50 μg/ml), PI (Propidium Iodide, 100 μg/ml) and Hoechst (10 μg/ml) at room temperature for 15 min in the dark. Cytoplasts were immediately examined by confocal microscopy.

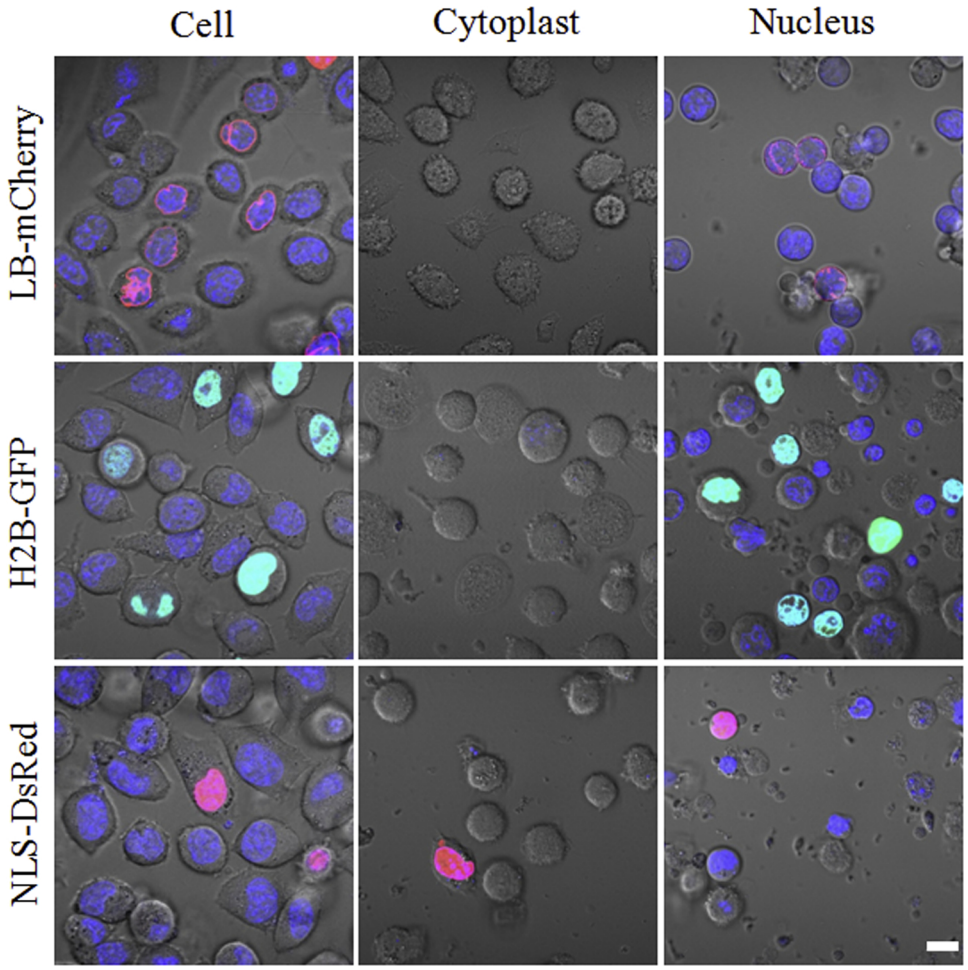

Fig. 5. Tracing of the nucleus after centrifugation. BMSCs were transfected with a plasmid carrying an expression cassette of Lamin B (LB)-mCherry, H2B-EGFP, or NLS-DsRed, which labels the nuclear lamina, histone and nucleoplasm, respectively. Cells were enucleated in ECM-coated glass-bottom 24-wells 48 h after transfection. After staining with Hoechst, cells, cytoplasts and recovered nuclei were examined by confocal microscopy. Scale bar = 10 μm.

2.12. Statistical analysis

All statistical analyses were performed using GraphPad Prizm 7. Error bars on boxplots represent the smallest and largest values, except that error bars on line graphs represent the SEM. The results were subjected to two-tailed Student's *t*-test and the one-way ANOVA with Tukey's post-hoc test. A p value less than 0.05 was considered statistically significant.

3. Results

3.1. ECM and colchicine increased enucleation efficiency

We first established a modified procedure for enucleation of animal cells (Fig.1. See Methods and figure legend for detail). As shown in Fig. 2, ECM increased the enucleation efficiency of BMSCs from about 60% to 70% in the presence of cytochalasin B. A much greater effect was achieved with colchicine, and supplementation of both ECM and colchicine increased the efficiency to about 98%. Similar results were found with BHKs. In addition, the volume of cytoplasts after 2 h recovery tended to be larger when ECM or colchicine was presence (Data not shown), suggesting less amount of cytoplasm was lost.

To test if this modified procedure could have a wider range of application, we carried out enucleation experiment on two human cell lines (HuMSCs and Ad293), which have a relatively poorer adhesion capability than BMSCs and BHKs (Fig.S1). A large quantity of cells detached in the absence of ECM, and the detachment was even worse in the presence of colchicine, making it difficult to quantify the enucleation rate. However, in the presence of ECM, enucleation of HuMSCs and Ad293 cells achieved 45% and 60% respectively. Further addition of colchicine increased enucleation efficiency to 80–85%, which however was still substantially lower than that of BMSCs and BHK cells (Fig. 2B).

3.2. Detection and measurement of ECM components

In addition to increase adhesion, ECM also stimulated proliferation in most of tested cells (Fig. S1). To investigate which components in ECM might be responsible for these effects, immunostaining, electrophoresis and proteomics analysis were carried out. As shown in Fig. 3A, HTB9 cells produced abundant fibronectin, which remained in the well after lysis with ammonia hydroxide. No residual nucleus signal was detected after lysis. Similar results were found with collagen I staining, although a weaker signal was detected (Data not shown).

ECM was then isolated, extracted and analyzed by electrophoresis (SDS-PAGE). The staining with Coomassie Blue revealed multiple prominent bands with molecular weight larger than 35 kD (Fig. 3B). Further, proteomics analysis of the isolated ECM was conducted by mass spectrometry. Within the top 15 Unused ProtScore, several ECM and cell-substrate interacting proteins, including laminin (α3, β3, γ2), plectin, integrin (β4, α6), annexin A2, and transforming growth factor-beta-induced protein ig-h3 (TGFBI) were identified (Fig. 3B, Table S1).

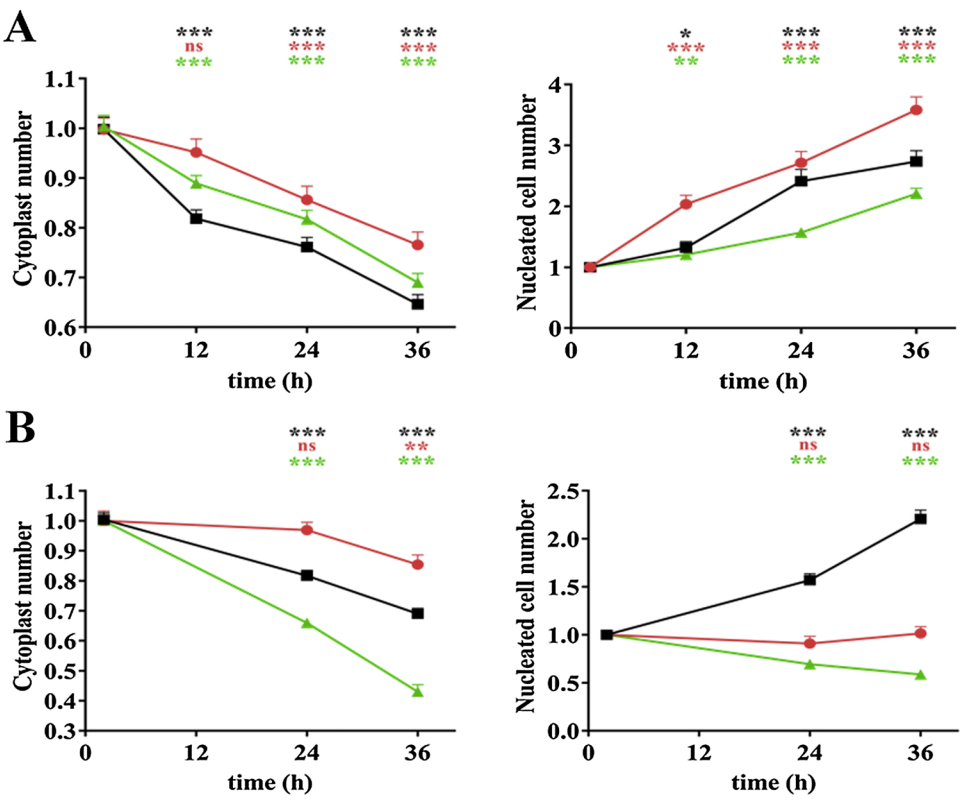

Fig. 6. Measurement of cytoplast viability. (A) BMSCs were seeded in a 24-well pre-coated with or without ECM and centrifuged in the presence or absence of colchicine. Cells were stained with Calcein and Hoechst and examined by confocal microscopy. Viable cytoplasts (Left) and nucleated cells (Right) as percentage of starting population over time are shown as mean ± SEM (n = 3 experiments). Student's *t*-test is performed between successive time points for either nucleated cells or cytoplasts. ***, $P < 0.001$; **, $P < 0.01$; *, $P < 0.05$. Black Square: uncoated; Red Circle: ECM-coated; Green Triangle: ECM-coated with colchicine. (B) BMSCs were seeded in 24-wells pre-coated with ECM and centrifuged in the presence of colchicine. After enucleation, cells were cultivated in medium supplemented with Paclitaxel (Taxol) or Doxorubicin (Dox). Cells were stained with Calcein and Hoechst and examined by confocal microscopy. Viable cytoplasts (Left) and nucleated cells (Right) as percentage of starting population over time are shown as mean ± SEM (n = 3 experiments). Student's *t*-test is performed between successive time points for either nucleated cells or cytoplasts. ***, $P < 0.001$; **, $P < 0.01$; *, $P < 0.05$. Black Square: Control; Red Circle: Taxol; Green Triangle: Dox.

3.3. Enucleation in glass-bottom well allowed direct confocal microscopy analysis

To facilitate direct confocal microscopy examination, we performed enucleation in glass-bottom wells. More than 90% efficiency was achieved when BMSCs were spun at 7000 rpm (6300 g) for 60 min. The reduced efficiency was probably due to less amount of ECM and thus a weaker adhesion force generated. Confocal microscopy analysis showed that mitochondria and lysosomes were presence in cytoplasts and did not seem to be affected by enucleation (Fig. 4). Cytoskeletons including microtubule and microfilament could also be detected after immunofluorescence staining. Microfilaments mostly restored polymeric configuration after recovery for 2 h. On the other hand, microtubules remained dissembled after withdrawal of colchicine for 2 h.

3.4. Nuclear envelope did not rupture during enucleation procedure

It has been reported that nuclear envelope was broken after centrifugation at high speed in a Ficoll density gradient (Graham et al., 2018). To test if this occurred in our procedure, the nuclear lamina, nucleoplasm and histone were labeled with lamin B-mCherry, NLS-DsRed (NLS: Nuclear Localization Signal) and H2B-EGFP, respectively, by gene transfection. We achieved about 18% labeling of lamin B. After enucleation, none of the cytoplasts showed fluorescence signal, indicating that no rupture of nuclear envelope occurred during centrifugation (Fig. 5). Further, the nuclei were recovered and examined by confocal microscopy. The result showed that about 18% of the recovered nuclei were labeled with lamin B-mCherry. Similar results were found when BMSCs were labeled with NLS-DsRed or H2B-EGFP.

For comparison, BMSCs and BHKs without ECM were spun at 11,000 RPM (15,500 g) for 60 min, which was similar to the classical coverslip method. Enucleation rate reached 94% for BMSCs and BHKs (Fig.S2), which was close to the efficiency by using the method established in this study (Fig. 2). However, most of BHKs detached from the 24-well (Fig.S2). When HuMSCs and Ad293 cells were used, no single cell remained in the well after high speed centrifugation. In addition, when BMSCs were transfected with a plasmid carrying the NLS-DsRed expression cassette, red fluorescence signal could be detected in a few cytoplasts after high speed centrifugation (Fig.S3), suggesting the occurrence of nuclear rupture. When NLS-DsRed labeled Ad293 cells were enucleated in a Ficoll gradient after high speed centrifugation, NLS-DsRed signal was detected in about 20% of cytoplasts (Data not shown).

3.5. ECM increased the survival of cytoplast

The survival of BMSC cytoplasts generated with or without ECM was examined by Calcein staining. The result showed that the presence of ECM greatly increased the number of viable cytoplasts at 36 h as compared to that of control ($p < 0.001$), while supplementation of colchicine reduced the survival rate as compared to that with ECM alone (Fig. 6A, $p < 0.05$). As expected, the remaining nucleated cells proliferated and increased in number during the experiment.

The death of cytoplasts was examined by confocal microscopy after staining with Annexin V-FITC, Propidine Iodine and Hoechst (Fig. S4). The result showed that cytoplasts died predominantly of apoptosis. Further, the presence of ECM significantly reduced the proportion of apoptosis, resulting in enhanced survival of cytoplasts.

3.6. Paclitaxel extended the lifespan of cytoplast

To eliminate the residual nucleated cells, paclitaxel or doxorubicin, two apoptotic inducers, was added into the culture after centrifugation. Indeed, addition of paclitaxel or doxorubicin resulted in decreased number of nucleated cells (Fig. 6B). Addition of doxorubicin also kill cytoplasts by apoptosis (Fig. 6B/7). Surprisingly, cytoplasts declined only slightly in the presence of paclitaxel at the first 24 h (Fig. 6B), and the number of viable cytoplasts at indicated time points was significantly higher than that of control ($p < 0.01$). It seemed that paclitaxel did not reduce apoptosis of cytoplasts (Fig. 7A); however, significantly less amount of floating apoptotic cells were observed in wells with paclitaxel (Data not shown), resulting in more viable cytoplasts (Fig. 7B). On the other hand, paclitaxel stimulated vacuolation in

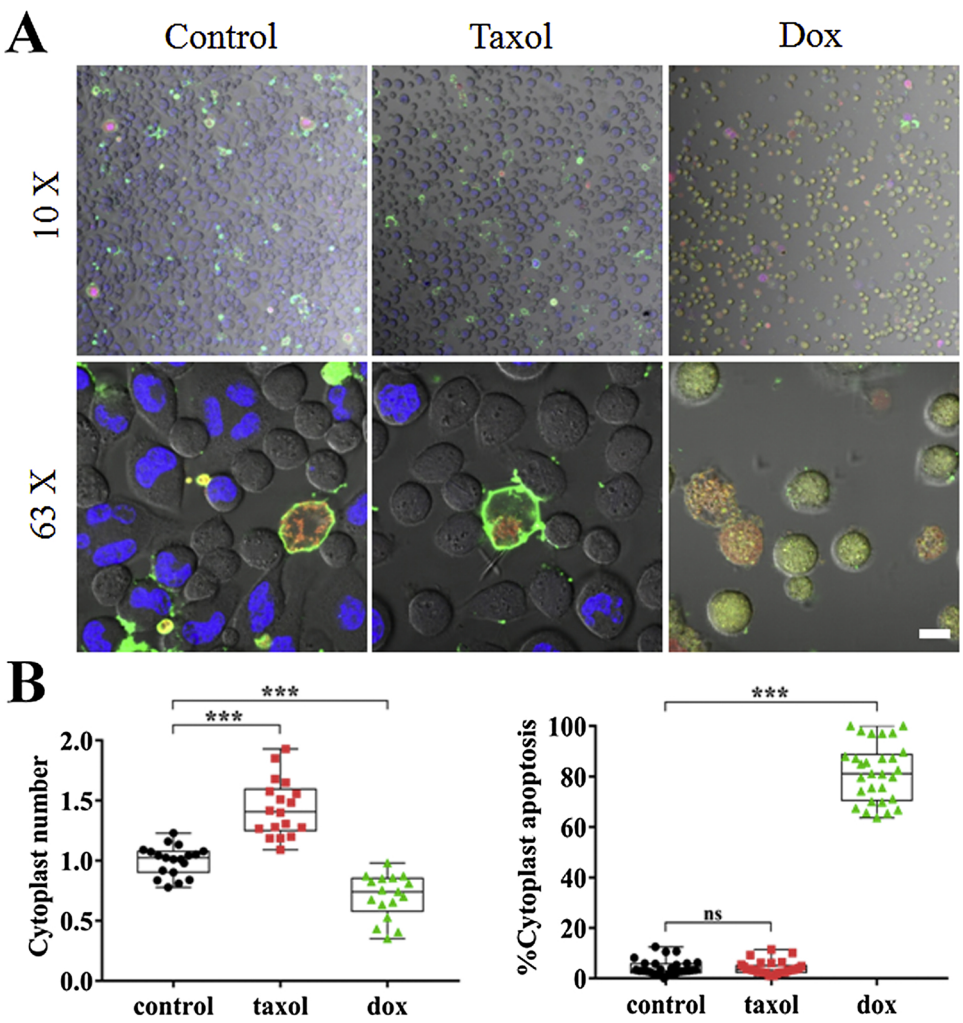

Fig. 7. Measurement of apoptosis in cytoplasts. BMSCs were enucleated in ECM-coated 24-wells in the presence of colchicine. (A) Cells were incubated in culture medium supplemented with or without paclitaxel (Taxol) or doxorubicin (Dox) for 36 h. Cells were harvested and stained with Annexin V-FITC, Propidium Iodide (PI) and Hoechst, and subsequently analyzed by confocal microscopy using 10X and 63X objective (Scale bar = 10 μm.). (B) Boxplots of viable cytoplast numbers (Left) and Annexin positive cytoplast percentage (Right). The control value was used as a reference. For cytoplasts: Control, n = 19; Taxol, n = 18; Dox, n = 17. For rate of apoptosis: Control, n = 29; Taxol, n = 29; Dox, n = 29. ***, $P < 0.001$; **, $P < 0.01$; *, $P < 0.05$.

cytoplasts (Fig.S5), suggesting the occurrence of paraptosis.

To understand how paclitaxel extended the lifespan of cytoplasts, we investigated the integrity of mitochondria, which is essential for induction of apoptosis. Staining with Mito-Tracker Green revealed elongated mitochondria in both nucleated cells and cytoplasts in the presence of paclitaxel (Fig. 8), suggesting the lack of dynamic fusion and fission of mitochondria. Further, staining with TMRE showed that paclitaxel increased while doxorubicin reduced significantly mitochondrial membrane potential. Moreover, staining with DCFH showed that doxorubicin dramatically increased cellular ROS levels; however, treatment with paclitaxel did not change ROS levels significantly.

4. Discussion

In the present study, we made several modifications to the cellular enucleation technique based on adherent cells on coverslip, which is not easy to handle and is not as suitable for cell culture. In our procedure, cells were cultivated in a 24-well, and a designed O-ring helped the 24-well positioned evenly in a 50-ml conical tube. Tilting of the 24-well never happened during centrifugation. On the other hand, unbalance of the coverslip could severely compromise enucleation efficiency. Even worse, tilting during centrifugation could lead to breaking of the glass coverslip.

The second modification was the adaption of ECM from HTB9 human bladder carcinoma cells, which has been used for the cultivation of islet beta-cells (Kaido et al., 2006). The presence of ECM clearly increased enucleation rate of BMSCs, BHKs and Ad293 cells (Fig. 2). On the contrary, we failed to detect any effect on enucleation when collagen, gelatin or poly-L-lysine was used for coating (Data not shown). Abundant cell-substrate interacting proteins were found in ECM (Fig. 3, Table S1), which could explain the increased adhesion and proliferation in most of tested cells (Fig.S1). In addition, ECM increased membrane fluidity of BHKs (Fig.S6), and modulation of membrane fluidity with H_2O_2 or DMSO could significantly influence enucleation rate (Fig.S7). Therefore, the results demonstrated that cell adhesion and membrane fluidity are two factors critical for cellular enucleation.

The third modification was the inclusion of colchicine for enucleation. Colchicine is a well-known microtubule polymerization inhibitor. Colchicine has also been shown to enhance enucleation of BMSCs (Ruan et al., 2008); however, colchicine has not been used routinely for cellular enucleation. Consistent with the previous report, we found colchicine dramatically increased enucleation rate of all tested cells, including BMSCs, BHKs, HuMSCs and Ad293. Therefore, supplementation of ECM and colchicine to cytochalasin B resulted in efficient cellular enucleation even at low centrifugation speed, which greatly facilitated the use of glass-bottom wells and subsequent detection of cellular organelles and structures by confocal microscopy (Fig. 4). Therefore, besides microfilaments, microtubes also affect cellular enucleation.

Further improvements could be made to the method reported in this study. ECM from HTB9 cells may not suitable for some other cells due to the limited protein species secreted. Reagents other than colchicine have also been reported to promote enucleation (Saito and Yamaguchi, 1988). The use of 24-well limited the number of cells that could be enucleated during each experiment. However, it is conceivable that a 6-well or 10-cm dish be used by simply changing the 50-ml conical tube

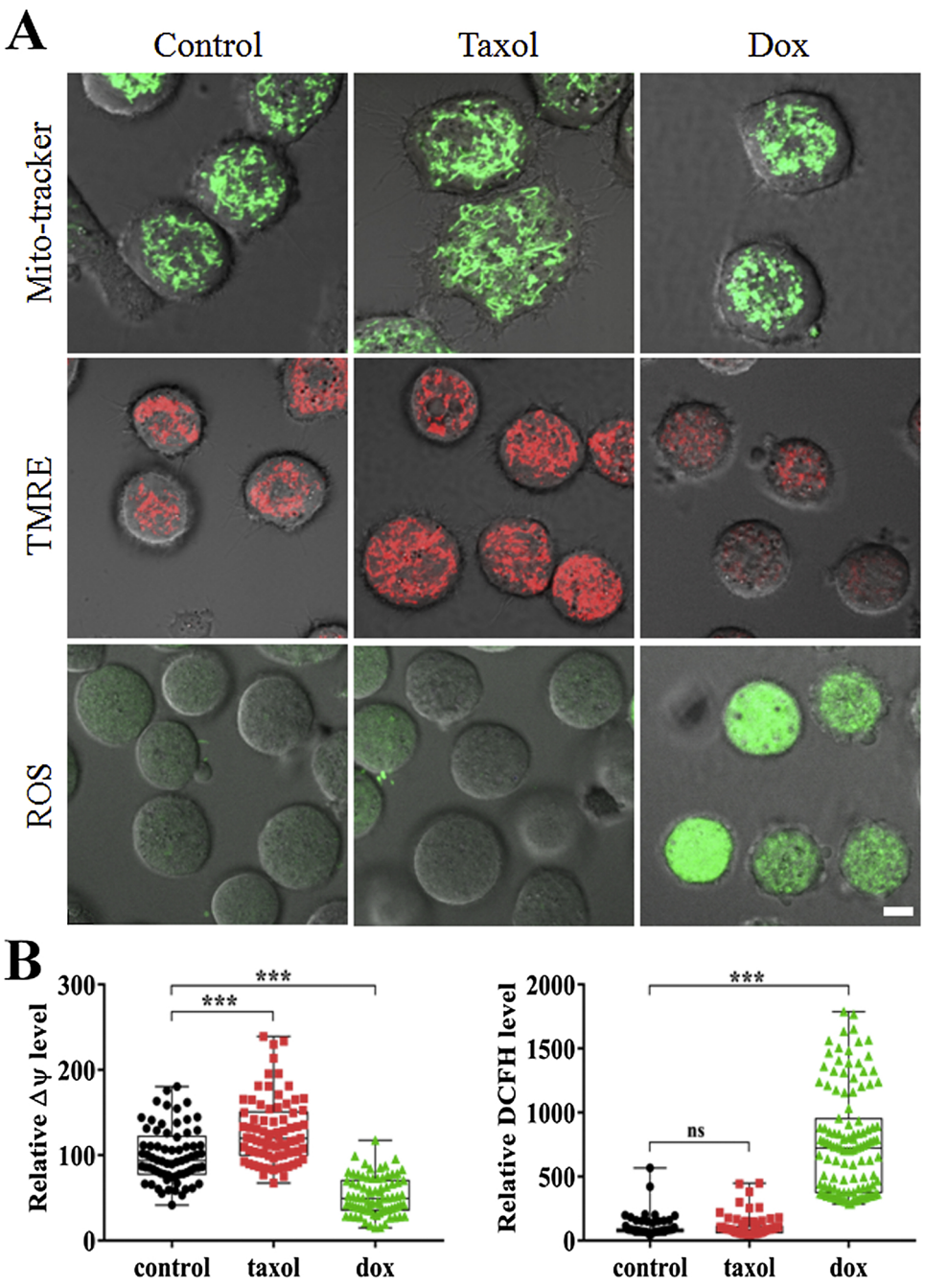

Fig. 8. Measurement of mitochondria structure, membrane potential and ROS levels. BMSCs were enucleated in ECM-coated 24-wells in the presence of colchicine. Cells were incubated in culture medium supplemented with or without paclitaxel (Taxol) or doxorubicin (Dox) for 24 h. (A) Cells were stained with Mito-Tracker Green, TMRE or DCFH-DA, and subsequently analyzed by confocal microscopy to reveal mitochondrial structure, membrane potential and ROS levels respectively. Scale bar = 5 μm. (B) Boxplots of relative mitochondrial membrane potential (Δψ) (Left) and ROS levels (Right). The control value was used as a reference. For membrane potential: Control, n = 70; Taxol, n = 79; Dox, n = 80. For ROS: Control, n = 81; Taxol, n = 74; Dox, n = 117. ***, $P < 0.001$; **, $P < 0.01$; *, $P < 0.05$.

to a larger utensil. Lastly, due to the limitation in our lab, we did not test enucleation with a swinging bucket rotor, which is predominantly used in previous reports.

Nuclear envelope rupture has been reported during cancer cell migration (Denais et al., 2016; Raab et al., 2016), which could result in uncontrolled exchange of nucleo-cytoplasmic content. Surprisingly, it has also been reported during cellular enucleation (Graham et al., 2018). After centrifugation, nuclear localized-tdTomato fluorescence protein was absence from the recovered karyoplasts but could be detected in the cytoplasts. In our study, we labeled the nuclear lamina, nucleoplasm, and histone H2B by transfection of respective genes of fluorescence proteins (Fig. 5). Although the transfection efficiencies were low, our result clearly demonstrated the presence of fluorescence signal from recovered karyoplasts but was not detectable in the cytoplasts. Rupture of nuclear envelope could potentially lead to DNA damage and release of DNA fragments into the cytoplasts, which might hamper the application of enucleation technique. The discrepancy was likely due to low centrifugation speed used in our experiment, because nuclear rupture could be detected, thought in low percentage, in adherent and suspension cells after high speed centrifugation (Fig.S2 and Data not shown).

Cytoplasts will eventually die without continuous supply of transcripts from the nucleus; however, ECM significantly improved the viability of BMSC cytoplasts (Fig. 6A). ECM components are well known for their survival enhancing ability. For example, laminins are important for neuronal attachment, viability and network formation (Hyysalo et al., 2017). On the other hand, colchicine is mildly toxic and thus addition of colchicine reduced the survival effect of ECM (Fig. 6B). However, the type of death for cytoplasts has not been formally identify (Galluzzi et al., 2018). It has been shown that extrinsic signal could induce apoptosis in cytoplasts (Schulze-Osthoff et al., 1994). Starvation and compounds that inhibit general transcription could also induce

apoptosis (Iurlaro et al., 2017; Bensaude, 2011). In the presence study, the results clearly demonstrated that the death of cytoplasts under uninduced conditions was predominantly apoptotic (Fig.S3, and Fig. 7).

Supplementation of paclitaxel and doxorubicin after centrifugation was initially intended to kill off residual nucleated cells. Indeed, both paclitaxel and doxorubicin completely blocked the mitotic activity of nucleated BMSCs (Fig. 6C). Surprisingly, the presence of paclitaxel dramatically enhanced the viability of cytoplasts up to 36 h. One obvious explanation is that paclitaxel, an anti-microtubule agent that stabilizes the microtubule network, offset the effect of colchicine, which certainly was not completely washed away from the cytoplasts. However, this is not enough to account for the survival enhancing capability of paclitaxel compared to that of ECM alone. Addition of paclitaxel resulted in less floating apoptotic cells compared with that of control (Data not shown), leading to higher numbers of viable adherent cytoplasts (Fig.6B/7B). On the contrary, doxorubicin induced dramatic apoptotic cell death; however, both Annexin V-FITC and Propidine Iodine signals were weak in cytoplasts (Fig. 7A). On the other hand, it has been shown that paclitaxel can induce paraptosis-like cell death, which is characterized by the cytoplasmic vacuolization (Sun et al., 2010). We did notice the appearance of prominent vacuoles in cytoplasts in the presence of paclitaxel (Fig.S4), which was not detected in the control or doxorubicin treated cytoplasts. We postulate that paraptosis is a slower cell death process compared to classical apoptosis, which might explain the extended survival of cytoplast when paclitaxel was presence.

Finally, we examined the state of mitochondria, whose functions are essential to the life and death of cells. It has been reported that paclitaxel induces mitochondrial biogenesis (Karbowski et al., 2001). In the present study, we found paclitaxel stimulated the formation of a tubular mitochondrial network (Fig. 8), an indication of lack of fusion and fission dynamics. In contrast, doxorubicin treatment led to mitochondria swelling and fragmentation, which is consistent with the induction of apoptosis (Fig. 7). Further, we found increased mitochondrial membrane potential in cytoplasts treated with paclitaxel as compared to that of control (Fig. 8). The result is consistent with the report by André et al. (2000; 2002), but contradictory to the observation reported by Maldonado et al (2010). However, the result was consistent with the measurement of ROS levels, which was significantly induced by doxorubicin and was unchanged in cytoplasts treated with paclitaxel (Fig. 8). The results collectively suggested that paclitaxel might enhance the survival of cytoplasts by perturbation of mitochondrial functions; however, the exact mechanism is still not completely understood.

In conclusion, we developed an improved cellular enucleation method, which achieved high enucleation rate in the presence of ECM, cytochalasin B and colchicine after low-speed centrifugation. Cytoplasts generated in this system had high viability, which is valuable for investigation of nucleocytoplasmic interaction.

Funding

This research was supported by the Li Ka Shing Foundation; the Natural Science Foundation of China (http://www.nsfc.gov.cn/ Grant No.30971665, 81172894,81370925); and the Education Department of Guangdong (http://www.gdhed.edu.cn/ Grant No. cxzd1123). Science and technology bureau of Shantou City (Grant No. 2016-30)

Declaration of Competing Interest

No competing financial interests exist.

Appendix A. Supplementary data

Supplementary material related to this article can be found, in the online version, at doi:https://doi.org/10.1016/j.ejcb.2019.151045.

References

André, N., Braguer, D., Brasseur, G., Gonçalves, A., Lemesle-Meunier, D., Guise, S., Jordan, M.A., Briand, C., 2000. Paclitaxel induces release of cytochrome c from mitochondria isolated from human neuroblastoma cells. Cancer Res. 60, 5349–5353.

André, N., Carré, M., Brasseur, G., Pourroy, B., Kovacic, H., Briand, C., Braguer, D., 2002. Paclitaxel targets mitochondria upstream of caspase activation in intact human neuroblastoma cells. FEBS Lett. 532, 256–260.

Bensaude, O., 2011. Inhibiting eukaryotic transcription: Which compound to choose? How to evaluate its activity? Transcription 2, 103–108.

Caron, J.M., Jones, A.L., Rall, L.B., Kirschner, M.W., 1985. Autoregulation of tubulin synthesis in enucleated cells. Nature 317, 648–651.

de Souza Carvalho, C., Kasmapour, B., Gronow, A., Rohde, M., Rabinovitch, M., Gutierrez, M.G., 2011. Internalization, phagolysosomal biogenesis and killing of mycobacteria in enucleated epithelial cells. Cell. Microbiol. 13, 1234–1249.

Denais, C.M., Gilbert, R.M., Isermann, P., McGregor, A.L., te Lindert, M., Weigelin, B., Davidson, P.M., Friedl, P., Wolf, K., Lammerding, J., 2016. Nuclear envelope rupture and repair during cancer cell migration. Science 352, 353–358.

Follett, E.A., Pringle, C.R., Wunner, W.H., Skehel, J.J., 1974. Virus replication in enucleate cells: vesicular stomatitis virus and influenza virus. J. Virol. 13, 394–399.

Galluzzi, L., Vitale, I., Aaronson, S.A., 2018. Molecular mechanisms of cell death: recommendations of the Nomenclature Committee on Cell Death 2018. Cell Death Differ. 25, 486–541.

Graham, D.M., Andersen, T., Sharek, L., Uzer, G., Rothenberg, K., Hoffman, B.D., Rubin, J., Balland, M., Bear, J.E., Burridge, K., 2018. Enucleated cells reveal differential roles of the nucleus in cell migration, polarity, and mechanotransduction. J. Cell Biol. 217, 895–914.

Hellewell, A.L., Rosini, S., Adams, J.C., 2017. A rapid, scalable method for the isolation, functional study, and analysis of cell-derived extracellular matrix. J. Vis. Exp. 119. https://doi.org/10.3791/55051.

Herbert, M., Turnbull, D., 2018. Progress in mitochondrial replacement therapies. Nat. Rev. Mol. Cell Biol. 19, 71–72.

Hyysalo, A., Ristola, M., Mäkinen, M.E., Häyrynen, S., Nykter, M., Narkilahti, S., 2017. Laminin α5 substrates promote survival, network formation and functional development of human pluripotent stem cell-derived neurons in vitro. Stem Cell Res. 24, 118–127.

Iurlaro, R., Püschel, F., León-Annicchiarico, C.L., O'Connor, H., Martin, S.J., Palou-Gramón, D., Lucendo, E., Muñoz-Pinedo, C., 2017. Glucose deprivation induces ATF4-mediated apoptosis through TRAIL death receptors. Mol. Cell. Biol. 37, e00479–16.

Kaido, T., Yebra, M., Cirulli, V., Rhodes, C., Diaferia, G., Montgomery, A.M., 2006. Impact of defined matrix interactions on insulin production by cultured human beta-cells: effect on insulin content, secretion, and gene transcription. Diabetes 55, 2723–2729.

Karbowski, M., Spodnik, J.H., Teranishi, M., Wozniak, M., Nishizawa, Y., Usukura, J., Wakabayashi, T., 2001. Opposite effects of microtubule-stabilizing and microtubule-destabilizing drugs on biogenesis of mitochondria in mammalian cells. J. Cell. Sci. 114, 281–291.

Lee, J.E., Yang, Y.M., Yuan, H., Sehgal, P.B., 2013. Definitive evidence using enucleated cytoplasts for a nongenomic basis for the cystic change in endoplasmic reticulum structure caused by STAT5a/b siRNAs. Am. J. Physiol. Cell Physiol. 304, C312–323.

Lin, H.P., Zheng, D.J., Li, Y.P., Wang, N., Chen, S.J., Fu, Y.C., Xu, W.C., Wei, C.J., 2016. Incorporation of VSV-G produces fusogenic plasma membrane vesicles capable of efficient transfer of bioactive macromolecules and mitochondria. Biomed. Microdevices 18, 41.

Maldonado, E.N., Patnaik, J., Mullins, M.R., Lemasters, J.J., 2010. Free tubulin modulates mitochondrial membrane potential in cancer cells. Cancer Res. 70, 10192–10201.

Mandic, A., Hansson, J., Linder, S., Shoshan, M.C., 2003. Cisplatin induces endoplasmic reticulum stress and nucleus-independent apoptotic signaling. J. Biol. Chem. 278, 9100–9106.

Prescott, D.M., Myerson, D., WaUace, J., 1972. Enucleation of mammalian cells with cytochalasin B. Exp. Cell Res. 71, 480–485.

Raab, M., Gentili, M., de Belly, H., Thiam, H.R., Vargas, P., Jimenez, A.J., Lautenschlaeger, F., Voituriez, R., Lennon-Duménil, A.M., Manel, N., Piel, M., 2016. ESC RT III repairs nuclear envelope ruptures during cell migration to limit DNA damage and cell death. Science 352, 359–362.

Ruan, C.J., Feng, W.S., Feng, Z.Q., Gu, P., Zhang, H.B., 2008. Preparation and activity of cytoplasts from bone marrow mesenchymal stem cells. J. Clin. Rehab. Tissue Eng. Res. 12 (43).

Saito, T., Yamaguchi, J., 1988. Enucleation of phagocytic cells with adenine, guanine, and their nucleosides in combination with centrifugation. Biol. Cell 63, 287–296.

Schulze-Osthoff, K., Walczak, H., Dröge, W., Krammer, P.H., 1994. Cell nucleus and DNA fragmentation are not required for apoptosis. J. Cell Biol. 127, 15–20.

Sun, Q., Chen, T., Wang, X., Wei, X., 2010. Taxol induces paraptosis independent of both protein synthesis and MAPK pathway. J. Cell. Physiol. 222, 421–432.

Wigler, M.H., Weinstein, I.B., 1975. A preparative method for obtaining enucleated mammalian cells. Biochem. Biophys. Res. Commun. 63, 669–674.

Xu, L.Q., Lin, M.J., Li, Y.P., Li, S., Chen, S.J., Wei, C.J., 2017. Preparation of plasma membrane vesicles from bone marrow mesenchymal stem cells for potential cytoplasm replacement therapy. J. Vis. Exp. 123. https://doi.org/10.3791/55741.

Yu, H., Koilkonda, R.D., Chou, T.H., Porciatti, V., Ozdemir, S.S., Chiodo, V., Boye, S.L., Boye, S.E., Hauswirth, W.W., Lewin, A.S., Guy, J., 2012. Gene delivery to mitochondria by targeting modified adenoassociated virus suppresses Leber's hereditary optic neuropathy in a mouse model. PNAS 109, E1238–E1247.